Analyst

PAPER

View Article Online
View Journal

Cite this: DOI: 10.1039/c6an00033a

A duplex DNA–gold nanoparticle probe composed as a colorimetric biosensor for sequence-specific DNA-binding proteins†

Junho Ahn, Yeonweon Choi, Ae-Ree Lee, Joon-Hwa Lee and Jong Hwa Jung*

Received 6th January 2016,
Accepted 15th February 2016

DOI: 10.1039/c6an00033a

www.rsc.org/analyst

Using duplex DNA–AuNP aggregates, a sequence-specific DNA-binding protein, SQUAMOSA Promoter-binding-Like protein 12 (SPL-12), was directly determined by SPL-12-duplex DNA interaction-based colorimetric actions of DNA–Au assemblies. In order to prepare duplex DNA–Au aggregates, thiol-modified DNA 1 and DNA 2 were attached onto the surface of AuNPs, respectively, by the salt-aging method and then the DNA-attached AuNPs were mixed. Duplex-DNA–Au aggregates having the average size of 160 nm diameter and the maximum absorption at 529 nm were able to recognize SPL-12 and reached the equivalent state by the addition of ~30 equivalents of SPL-12 accompanying a color change from red to blue with a red shift of the maximum absorption at 570 nm. As a result, the aggregation size grew to about 247 nm. Also, at higher temperatures of the mixture of duplex-DNA–Au aggregate solution and SPL-12, the equivalent state was reached rapidly. On the contrary, in the control experiment using Bovine Serum Albumin (BSA), no absorption band shift of duplex-DNA–Au aggregates was observed.

Introduction

The detection of sequence-specific DNA-binding proteins is crucial to elucidate gene expression mechanisms and cellular function because of their important roles in transcriptional regulatory networks including transcription, replication, recombination and repair.[1–4] Moreover, these proteins have long been recognized as attractive markers or targets for disease diagnosis and drug development.[5,6] Thus, the development of rapid, simple and robust strategies for detecting sequence-specific DNA-binding proteins and probing their DNA-binding activities is of paramount importance in biological fields such as proteomics, genomics and biomedicine. Conventional approaches for sequence-specific DNA-binding proteins, including the electrophoretic mobility shift assay and the DNase footprinting assay, are well-known.[7–9]

One method for the determination of sequence-specific DNA-binding proteins is using dye-labeled DNA–AuNPs. Specific interactions between DNA and proteins which induce structural or geometrical modification of DNA lead to a turn-on type fluorescence signal of the dye.[10,11] For example, in the presence of the target protein, DNA was dissociated from the surface of AuNPs because of the competitive binding, resulting in salt-induced aggregation of the AuNPs which enables colorimetric analysis and fluorescence analysis.[12] Prof. N. O. Reich *et al.* have investigated the detection of sequence-specific protein–DNA interactions through surface enhanced resonance Raman scattering. They used silver-plated DNA and gold nanoparticle assemblies to identify sequence-specific and concentration-dependent binding of a DNA cytosine-C5-methyltransferase and the eukaryotic transcriptional regulator, TATA binding protein.[13] However, these methods are not only laborious and time-consuming, but also require radioisotope or fluorescence labels. Thus, there is still a need for the development of inexpensive and simple methods for the detection of sequence-specific DNA-binding proteins. Furthermore, Huang *et al.* have reported colorimetric determination of proteins using aptamer-modified gold nanoparticles. But, in the mixture of aptamer–AuNPs with an excess amount of protein in solution, it was hard to detect colorimetric signals with their system.[14] Most systems using DNA–AuNPs for colorimetric detection of sequence-specific DNA-binding proteins use supporting proteins such as *endo-* or *exo* nucleases which are able to distinguish stabilized protein–duplex DNA–AuNP conjugates.[15–18] In addition, Prof. R.-Q. Yu *et al.* also reported a novel exonuclease III protection-based colorimetric biosensing system using DNA-cross-linked gold nanoparticles.[19] These modified gold nanoparticles were found to recognize the TATA binding protein.

Department of Chemistry and Research Institute of Natural Sciences, Gyeongsang National University, Jinju 660-701, Korea. E-mail: jonghwa@gnu.ac.kr

†Electronic supplementary information (ESI) available: The TEM images, IR spectra, UV-Vis spectra, photographs of duplex DNA–Au and DNA–Au-2, DLS measurements, CD spectra, and ^{1}H NMR spectra. See DOI: 10.1039/c6an00033a

Functionalized gold nanoparticles are of great interest for biomedical and environmental research applications such as bioseparations, drug targeting, cell isolation, enzyme immobilization and protein purification because of their biocompatibility.[20–22] In particular, gold nanoparticles are easily modified by chemically linking DNA to the surface of the nanoparticles with a thiol terminal group. In addition, DNA functionalized gold nanoparticles can be controlled as duplex and triplex strand DNA structures by complementary interaction with base pairs.

In this context, SQUAMOSA promoter-binding-like protein 12 (SPL-12) was selected as a specific DNA-binding protein. SPL genes have been shown to play numerous important roles during plant growth and development.[23] SPL have been discovered in a wide array of terrestrial plants, from green algae, moss, to silver birch, tomato, rice and maize.[24] In particular, SPL-12 protein consists of 124 amino acids.[25] SQUAMOSA promoter-binding-like proteins form a major family of plant-specific transcription factors, mainly related to flower development.[23,24,26] Among the amino acids in SPL-12, positively charged Arg and Lys side-chains not only bind to a negatively charged DNA backbone through electrostatic attraction, but are also capable of recognizing bases by forming hydrogen bonds.[26,27] If the quantitative detection of SPL-12 in plants can be rapidly performed by a simple and convenient method, the growth rate of plants can be monitored and controlled. The selective binding affinity of SPL-12 to duplex DNA formed by GGCATGT and CCGTACA sequences has been reported.[25,27] Several conserved residues in SPL-12, such as Lys17, Arg/Lys21, Arg22, and Lys/Arg24 are involved in the binding of SPL-12 to the duplex DNA by electrostatic and hydrogen bond interactions with the DNA sequences. Thus, the duplex DNA consisting of GGCATGT and CCGTACA would be useful for detecting SPL-12.[27,28]

Herein, we developed a novel and convenient colorimetric biosensing strategy for detecting the sequence-specific DNA-binding (SPL-12) protein. This strategy relied on the DNA-cross-linked AuNP aggregation by specific interactions of SPL-12 with the AuNP-linked DNA binding sequences. To the best of our knowledge, this strategy is a rare example of a colorimetric biosensor for visual detection of a sequence-specific DNA-binding protein. We herein report the first example capable of detecting the SPL-12 protein using DNA–Au nanoparticles based on colorimetric signal changes induced by the size effect of duplex-DNA–Au nanoparticles without supporting materials such as *exo* or *endo*-nucleases. This detecting method could be more cost-effective, simpler and faster in detecting SPL-12 than the electrophoresis assay which is the most used method to detect the SPL-12 protein. This system is comprised of two Au nanoparticles, each possessing a different sequence of DNA. The one DNA–Au type consists of gold nanoparticles conjugated with a thiol-end group at the 5′ terminal group containing CCGTACA, in which the sequence is 5′ to 3′. The other DNA–Au type consists of gold nanoparticles conjugated with a thiol-end group at the 5′ terminal group containing TGTACGG.

Experimental

Materials and instruments

All DNAs were purchased from Bionics. $HAuCl_4$, tris(2-carboxyethyl)phosphine hydrochloride (TCEP), trisodium citrate, Bovine Serum Albumin (BSA), myoglobin, egg white albumin, lysozyme and Human Serum Albumin(HSA) were purchased from Sigma-Aldrich. NaCl, Na_2HPO_4 and NaH_2PO_4 were purchased from Samchun Pure Chemicals. A UV–Vis spectrophotometer (Thermo Evolution 600; Thermo Fisher Scientific, Waltham, MA, USA) was used to obtain the absorption spectra. A Transmission Electron Microscope (TEM) which was operated at 200 kV was used to obtain images and morphologies of nanoparticles (JEM2010; Jeol, Tokyo, Japan). To measure the size of the nanoparticles, Dynamic Light Scattering (DLS) experiments were carried out at 25 °C (NANO ZS; Malvern, Westborough, MA, USA). A FT-IR spectrophotometer was used to confirm the DNA attachments on the surface of nanoparticles (Shimadzu FT-IR 8400S; Shimadzu, Kyoto, Japan). CD spectra were obtained using a Jasco J-815 CD spectrophotometer.

Preparation of Au nanoparticles

An aqueous solution of $HAuCl_4$ (1 mM, 500 mL) was brought to a reflux while stirring, and then 50 mL of a 38.8 mM trisodium citrate solution was added quickly, which resulted in a change in the solution color from pale yellow to deep red. After the color change, the solution was refluxed for an additional 10 min, allowed to cool to room temperature, and subsequently filtered through a membrane; 0.45 μm nylon filter.

Fabrication of DNA–Au-1 and DNA–Au-2

Thiolated DNAs were treated with TCEP (1 μM) at pH 5.0 for 1 hour to cleave the disulfide bond. The activated DNA was desalted using a C18 Sep-Pak column and lyophilized. The dried 20 nmol of DNAs were mixed with 0.2 nmol AuNP solutions respectively. NaCl was added to the AuNP solution containing DNAs; the final concentration of NaCl was 0.1 M. The AuNP solutions were stirred for 1 day at room temperature. The unlinked DNAs were removed by centrifugation at 16 000 rpm for 30 minutes. **DNA–Au-1** or **DNA–Au-2** solution was redispersed in 10 mM phosphate buffer pH 7.0 containing 0.1 M NaCl.

Preparation of SPL-12

The coding sequence DNAs for site-directed mutagenesis were purchased from BIONEER Inc. (Korea) and were cloned into the *Escherichia coli* expression vector pET28a with an N-terminal His-tag (Novagen, WI, USA), and the expression vectors were used to transform the *E. coli* strain BL21 (DE3). Uniformly ^{15}N-labeled SPL-12 mutants were obtained by growing the transformed *Escherichia coli* cells in M9 medium that contained 1 g L^{-1} $^{15}NH_4Cl$. The ^{15}N-labeled mutant SPL-12 proteins were purified with a Ni–NTA affinity column and a Sephacryl S-100 gel filtration column (GE Healthcare, USA) on

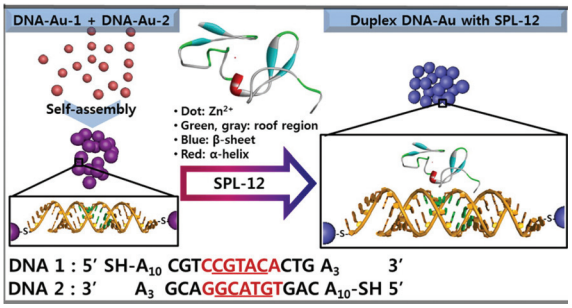

Scheme 1 Representation for sensing of SPL-12 using the duplex DNA–Au nanoparticles.

a GE AKTA Prime Plus as described elsewhere. The SPL-12 protein was dissolved in 20 mM Trsi-HCl (pH 7.5), 300 mM NaCl, 20 μM EDTA, 100 μM $ZnCl_2$, and 5 mM 2-Mercapto ethanol.[23]

Preparations of duplex DNA–Au and protein recognition

Equal volume of **DNA–Au-1** and **DNA–Au-2** was mixed. This solution was stirred for 4 hours at room temperature. In the experiment for sensing of proteins, the concentration of duplex DNA–Au was 1 nmol. SPL-12 (20 equivalent) was added with a minimal volume into the duplex DNA–Au solution.

The overall synthetic procedure for functionalized Au nanoparticles is depicted in Scheme 1. First, we prepared the supporting nanomaterials from the Au nanoparticles of *ca.* 12 nm particle diameter by a previously reported procedure.[29] Then, thiol-functionalized DNA 1 (5′-SH-A10 CGT CCGTACA CTG A3-3′) was attached to gold nanoparticles in 0.1 M NaCl aqueous solution under stirring overnight.[30] The DNA-functionalized gold nanoparticles (**DNA–Au-1**) were collected by centrifugation. The other thiol-functionalized DNA 2 (3′-A3 GCA GGCATGT GAC A10-SH-5′) were also attached to gold nanoparticles (**DNA–Au-2**) and the DNA–Au particles (**DNA–Au-1** and **DNA–Au-2**) were characterized by transmission electron microscopy (TEM) and FT-IR spectroscopy.

Results and discussion

The TEM images of **DNA–Au-1** and **DNA–Au-2** revealed a spherical structure with a narrow size distribution (*ca.* 12 nm) (Fig. 1A and S1†). The IR result was in accord with bond formation; the IR spectra of DNA 1 and 2 showed strong new bands at 1727, 1634, 1521, 1408 and 1336 cm^{-1} which originated from the receptor DNA, in accordance with the DNA now residing on the Au nanoparticles (Fig. S2†).

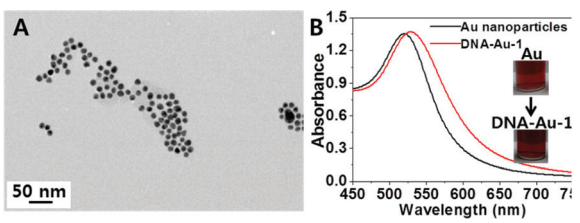

Fig. 1 (A) TEM image of **DNA–Au-1**, and (B) UV-Vis spectra of Au and **DNA–Au-1**.

Spectroscopic measurements of both **DNA–Au-1** and **DNA–Au-2** nanoparticles were performed in 10 mM phosphate buffer pH 7.0 with 0.1 M NaCl. The UV-vis absorption spectrum of **DNA–Au-1** nanoparticles showed one absorption band at 529 nm with red color (Fig. 1B). **DNA–Au-1** nanoparticles themselves can be aggregated *via* hydrogen bonding interactions between DNA sequences such as A–T and C–G. Three intermolecular hydrogen-bonding interactions were possible in **DNA–Au-1**, which would induce a short red-shift. The absorbance of the solution of **DNA–Au-1** nanoparticles was constant over time (Fig. S3A†), indicating that the **DNA–Au-1** nanoparticles did not aggregate. In addition, the absorption band of the **DNA–Au-2** nanoparticles was observed in the same visible range under the same conditions (Fig. S3B†).

In a typical experiment for duplex aggregation between the **DNA–Au-1** and **DNA–Au-2** nanoparticles, 10 nM of **DNA–Au-2** nanoparticle was added to the **DNA–Au-1** nanoparticle solution (10 nM) prepared at pH 7.0. The mixed sample appeared red with a UV-Vis absorption maximum at *ca.* 529 nm. When they were mixed, the DNA sequences on the two nanoparticles hybridized to form a DNA duplex and brought the particles in proximity. No significant color changes of **DNA–Au-1** and duplex DNA–Au were observed (Fig. S4†), but absorbance of mixed solution between **DNA–Au-1** and **DNA–Au-2** gradually decreased and reached equilibrium within 80 minutes (Fig. 2A). In a control experiment, we also observed the color of a mixed solution of **DNA–Au-1** nanoparticles and bare Au nanoparticles under the same conditions. No notable color change was observed but a slight absorbance decrease was observed. This was because of the result of interactions between citrate and DNA (Fig. S5†). To measure the average size of **DNA–Au-1** and **DNA–Au-2**, DLS was used. **DNA–Au-1** (22 nm) and **DNA–Au-2** (12 nm) showed a significant difference in Fig. S6,† because DNA 1 had one more T sequence than DNA 2 did, which can interact with the poly A sequence.

To gain more detailed structural information with respect to the duplex aggregation in a mixed solution of both **DNA–Au-1** and **DNA–Au-2** nanoparticles, we investigated the DNA-induced assembly processes by TEM. The TEM images of **DNA–Au-1** solution upon addition of **DNA–Au-2** suspension are shown in Fig. 2B. The TEM image of the mixture of both **DNA–Au-1** and **DNA–Au-2** at pH 7.0 showed a relatively less strong aggregate, because DNA 1 and DNA 2 possessed the poly A sequence which can cause stabilization of the Au nanoparticles. As a result, strong aggregation by the formation of duplex DNA–Au might not be possible. We also determined the aggregate nanoparticle size in a mixed solution of both **DNA–Au-1** and **DNA–Au-2** at pH 7.0 by DLS. The average diameters of the aggregate size in solution increased from 12 nm to 160 nm (Fig. S6 and S7†). On the other hand, the average diameters of a mixture of both **DNA–Au-1** and bare Au nanoparticles did not change (Fig. S8†). These findings suggest that

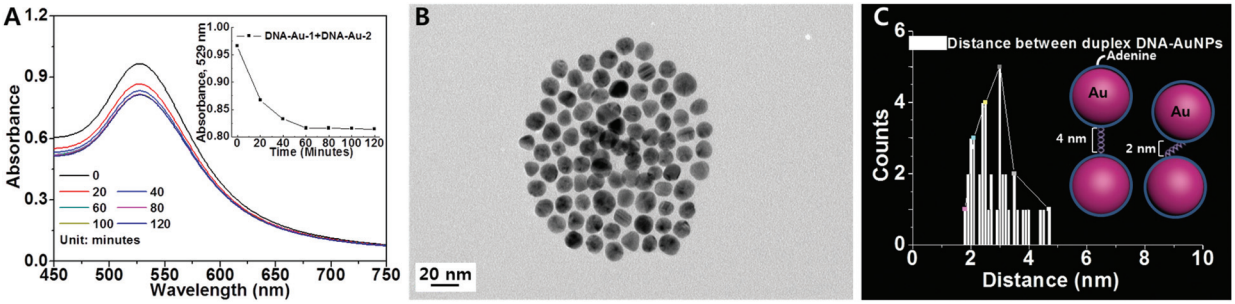

Fig. 2 (A) UV-Vis spectra of aggregation between **DNA–Au-1** and **DNA–Au-2** nanoparticles and changes of absorbance at 529 nm over time, (B) TEM image of a mixture solution of both **DNA–Au-1** and **DNA–Au-2**, and (C) depiction of duplex DNA–Au formation and their distances between **DNA–Au-1** and **DNA–Au-2**. These distances were measured from Fig. 2B.

the **DNA–Au-1** nanoparticles were aggregated with the **DNA–Au-2** nanoparticles by duplex formation. Furthermore, the average distances between **DNA–Au-1** and **DNA–Au-2** were 2–4 nm (Fig. 2D), which is consistent with the duplex distance between the DNA–Au nanoparticles in Fig. 2B. This distance was shorter than that of the length of DNA-1 or DNA-2 attached on the Au nanoparticles, because 10 adenosine moieties of DNA-1 or DNA-2 would be wrapped onto the surface of Au particles.[31,32] The distance smaller than 2 nm between nanoparticles in Fig. 2B proposed that the nanoparticles were put toward the *z*-axis orientation.

We observed the binding ability of the duplex DNA–Au nanoparticles prepared by both **DNA–Au-1** and **DNA–Au-2** nanoparticles for the SPL-12 protein. As shown in Fig. 3A, the UV-Vis absorption spectra of the solution were obtained at regular time intervals (every 10 min). The absorption band of the duplex DNA–Au nanoparticles was changed gradually from 529 nm to 562 nm upon addition of SPL-12. In contrast, the UV-Vis absorption wavelength in the duplex DNA–Au nanoparticles did not change upon addition of an excess of BSA solution (Fig. 3B), but the absorbance of the duplex DNA–Au upon addition of BSA decreased with time. This was because the positively charged amino acid in the BSA interacted with the negatively charged phosphate group of DNA. However this BSA–DNA interaction was not strong enough to change the distance between Au nanoparticles. Moreover, we performed further control experiment using myoglobin, egg white albumin, lysozyme and HSA (Fig. 3C and S9†). As shown in Fig. 3C and S9,† no significant absorbance and wavelength changes were observed. These results indicate that SPL-12 is bound to the duplex DNA–Au nanoparticles (Fig. 3C). As shown in Fig. S10,† the SPL-12 induced no wavelength shift of the duplex DNA–Au nanoparticles which consisted of **DNA–Au-3** (DNA 3: SH-CCC AGG TTC TCT AAA AAA AAA) and **DNA–Au-4** (DNA 4: SH-ACG CAT CTG TGA TTT TTT TTT), indicating that specific sequences of the duplex DNA–Au nanoparticles recognized the SPL-12 protein. It is well-known that the SPL-12 protein is selectively bound to the duplex DNA formed by both GGCATGT and CCGTACA sequence DNA.[21] Thus, the red shift is due to aggregation between the duplex DNA–Au nanoparticles upon the binding of SPL-12 to the specific DNA-binding sequence.

Furthermore, the UV-Vis absorption wavelength changes of the duplex DNA–Au nanoparticles were observed upon five different concentrations of addition of SPL-12 with 10 min interval (Fig. 4A). It was clear that, with low SPL-12 concentration (5 nmol), we observed the least red shift. When 30 nmol of SPL-12 was added to the duplex DNA–Au nanoparticle solution, we observed the largest red shift of the UV-Vis absorption band. The red shift of the duplex DNA–Au nanoparticles reached equilibrium after 80 min, displaying an absorption wavelength maximum at *ca.* 578 nm. This red shift

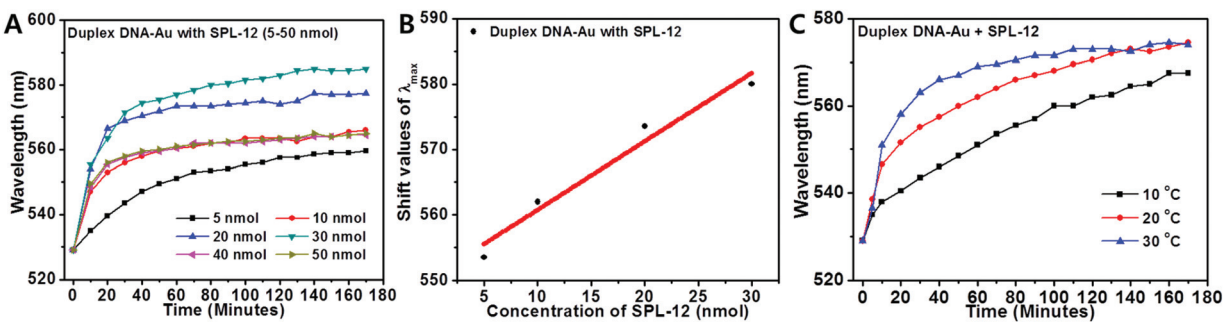

Fig. 3 (A) Change of λ_{max} values over time of the duplex DNA–Au (1 nmol) upon addition of different concentration of SPL-12 (5–50 nmol), (B) change of λ_{max} values over the concentration of SPL-12 of the duplex DNA–Au (1 nmol). Shift values of Fig. 4A at 80 minutes were selected, and (C) change of λ_{max} values over time of the duplex DNA–Au (1 nmol) involved SPL-12 (10 nmol) at different temperatures.

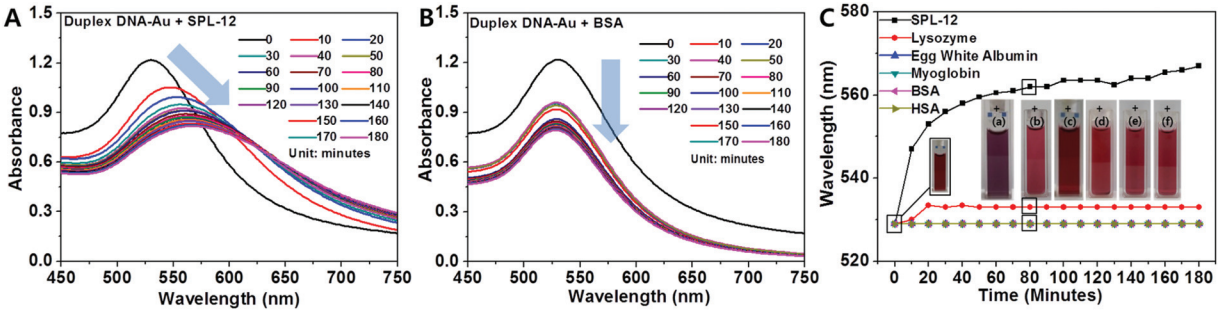

Fig. 4 (A) UV-Vis spectra of duplex DNA–Au (1 nmol) upon addition of SPL-12 (10 nmol), (B) time dependent UV-Vis spectra change of duplex DNA–Au (1 nmol) upon addition of BSA (10 nmol), and (C) plots of maximum absorption wavelengths shown in Fig. 3A, B and S10,† respectively, and photographs of the duplex DNA–Au (1 nmol) upon addition of SPL-12 (10 nmol), BSA (10 nmol), myoglobin (10 nmol), egg white albumin (10 nmol), lysozyme (10 nmol) and HSA (10 nmol), respectively.

of the duplex DNA–Au nanoparticles may be attributed to specific aggregation between the duplex DNA–Au nanoparticles and SPL-12 by specific intermolecular hydrogen-bonding interactions. In order to quantify detection ability of SPL-12, the graph plotting the wavelength shift *vs.* the concentration of SPL-12 (5–30 nmol) showed a good linearity (R^2 = 0.95) as shown in Fig. 4B.

We also observed changes in the absorption wavelength of the duplex DNA–Au nanoparticles upon addition of SPL-12 at three different temperatures (Fig. 4C). The absorption wavelength of the duplex DNA–Au nanoparticles showed the largest red shift upon addition of SPL-12 at 30 °C, which was attributed to the facile binding of SPL-12 to the C–G pocket in the duplex DNA–Au nanoparticles due to weak intermolecular hydrogen-bonding interactions between the C and G base pairs. The shift of the maximum absorbance wavelength to 570 nm occurred most quickly in the duplex DNA–Au nanoparticles upon addition of SPL-12 at the highest temperature of 30 °C.

To gain more detailed structural information with respect to the aggregated state of a mixed solution of the duplex DNA–Au nanoparticles with SPL-12, we investigated the DNA-induced assembly process by TEM. Unlike the TEM image of the duplex DNA–Au, the TEM image of a mixed solution of both the duplex DNA–Au and SPL-12 showed a different size distribution, which consisted of larger nanoparticles of *ca.* 250 nm (Fig. S11 and S12A†). This result indicates that the duplex DNA–Au nanoparticles were bound to SPL-12 by intermolecular hydrogen-bonding interactions. Thus, the TEM data were consistent with the UV-Vis absorption data. Through the data related with binding between SPL-12 and the duplex DNA–Au, we proposed a binding mechanism of the duplex DNA–Au with SPL-12. SPL-12 first binds to the duplex DNAs having relatively large inter-nanoparticle distances (>4 nm) out of the nanoparticles composed of duplex DNA–Au aggregates to form complexes. As a result, two nanoparticles getting closer made the distance between the nanoparticles increase, by which steric crowding decreased. Therefore, the interaction between SPL-12 and the duplex DNA–Au became stronger to facilitate aggregation of the duplex DNA–Au.

Furthermore, the duplex DNA–Au and the duplex DNA–Au nanoparticles appeared to be connected. To further evaluate the performance and consistency of our assay, we also determined the aggregate nanoparticle size in mixed solutions of the duplex DNA–Au upon addition of SPL-12 and BSA by DLS. The average diameters of the aggregate sizes in a mixed solution of the duplex DNA–Au nanoparticles with SPL-12 increased from 160 nm to 247 nm. In contrast, the average diameter of a mixture of the duplex DNA–Au with BSA was almost the same as that without BSA (Fig. S12B†). These findings suggest that SPL-12 was bound to the duplex DNA–Au nanoparticles.

To confirm the helicity of the duplex DNA, CD spectra of duplex DNA with and without SPL-12 were observed. The CD spectrum of duplex DNA without SPL-12 exhibited a positive sign for the first cotton effect, indicating that the DNA strands in duplex DNA were orientated in left-handed helicity. Upon addition of SPL-12 into the duplex DNA solution, no changes in the helicity and CD intensity occurred (Fig. S13†). These results strongly support the view that the helicity of duplex DNA was stable in the presence of SPL-12.

To further understand binding between a duplex DNA and SPL-12, the ^{1}H NMR spectrum of duplex DNA was observed upon addition of SPL-12. As shown in Fig. S14,† the imino proton resonances were assigned.[33] The imino proton resonances in the G bases were shifted to high field in the presence of SPL-12, indicating that SPL-12 could be bound to the C–G base pairs.

Conclusions

We have demonstrated the aggregation between DNA-functionalized gold nanoparticles composed of different DNA sequences. Two gold nanoparticles composed of different DNA sequences formed the duplex DNA structure by complementary interaction between mainly C and G at pH 7. The duplex DNA Au nanoparticles selectively recognized the SPL-12 protein, in which SPL-12 would be bound to the C–G base

pairs. In contrast, the duplex DNA–Au nanoparticles did not bind to the BSA protein. We expect that this strategy may offer a new approach for developing low cost sensitive systems that display selective detection of specific biomolecules. This new species of nanoparticles may be highly useful in a wide range of applications in biology, biomedicine, process control, and nanotechnology.

Acknowledgements

This work was supported by a grant from NRF (2014M2B2A9030338 and 2015R1A2A2A05001400). In addition, this work was partially supported by a grant from the Next-Generation BioGreen 21 Program (SSAC, grant#: PJ01117702), Rural development Administration, Korea.

Notes and references

1 B. Ren, F. Robert, J. J. Wyrick, O. Aparicio, E. G. Jennings, I. Simon, J. Zeitlinger, J. Schreiber, N. Hannett, E. Kanin, T. L. Volkert, C. J. Wilson, S. P. Bell and R. A. Young, *Science*, 2000, **290**, 2306.
2 S. T. Durant and J. A. Nickoloff, *Cell Cycle*, 2005, **4**, 1216.
3 A. Aboussekhra, M. Biggerstaff, M. K. K. Shivji, J. A. Vilpo, V. Moncollin, V. N. Podust, M. Protić, U. Hübscher, J. Egly and R. D. Wood, *Cell*, 1995, **80**, 859.
4 A. Kar, M. Kaur, T. Ghosh, M. M. Khan, A. Sharma, R. Shekhar, A. Varshney and S. Saxena, *Nucleic Acids Res.*, 2015, **43**, 4962.
5 P. P. Pandolfi, *Oncogene*, 2001, **20**, 3116.
6 D. Kim, Y. Lee, H. Hwang, K. K. Kim and H. Park, *Curr. Drug Targets*, 2010, **11**, 335.
7 M. M. Garner and A. Revzin, *Nucleic Acids Res.*, 1981, **9**, 3047.
8 D. J. Galas and A. Schmitz, *Nucleic Acids Res.*, 1978, **5**, 3157.
9 T. Moss and B. Leblanc, *DNA-Protein Interactions*, Humana Press, 2009.
10 W. Wang, C. Chen, M. Qian and X. S. Zhao, *Anal. Biochem.*, 2008, **373**, 213.
11 F. Li, H. Zhang, C. Lai, X. Li and X. C. Le, *Angew. Chem., Int. Ed.*, 2012, **51**, 9317.
12 W. Sun, Y. Lu, J. Mao, N. Chang, J. Yang and Y. Liu, *Anal. Chem.*, 2015, **87**, 3354.
13 A. J. Bonham, G. Braun, I. Pavel, M. Moskovits and N. O. Reich, *J. Am. Chem. Soc.*, 2007, **129**, 14572.
14 C. Huang, Y. Huang, Z. Cao, W. Tan and H. Chang, *Anal. Chem.*, 2005, **77**, 5735.
15 Z. Wang, R. Lévy, D. G. Fernig and M. Brust, *J. Am. Chem. Soc.*, 2006, **128**, 2214.
16 X. Xu, M. S. Han and C. A. Mirkin, *Angew. Chem., Int. Ed.*, 2007, **46**, 3468.
17 Y. N. Tan, X. Su, E. T. Liu and J. S. Thomsen, *Anal. Chem.*, 2010, **82**, 2759.
18 T. Gao, L. Ning, C. Li, H. Wang and G. Li, *Anal. Chim. Acta.*, 2013, **188**, 171.
19 L. Ou, P. Jin, X. Chu, J. Jiang and R. Yu, *Anal. Chem.*, 2010, **82**, 6015.
20 K. Cho, X. Wang, S. Nie, Z. Chen and D. M. Shin, *Clin. Cancer. Res.*, 2008, **14**, 1310.
21 C. Liu, Y. Hsieh, C. Huang, Z. Lin and H. Chang, *Chem. Commun.*, 2008, **19**, 2242.
22 J. Choi, Y. Jun, S. Yeon, H. C. Kim, J. Shin and J. Cheon, *J. Am. Chem. Soc.*, 2006, **128**, 15982.
23 J. C. Preston and L. C. Hileman, *Front. Plant Sci.*, 2013, **4**, 80.
24 X. Chen, Z. Zhang, D. Liu, K. Zhang, A. Li and L. Mao, *J. Integr. Plant. Biol.*, 2010, **52**, 946.
25 G. Cardon, S. Höhmann, J. Klein, K. Nettesheim, H. Saedler and P. Huijser, *Gene*, 1999, **237**, 91.
26 C. O. Pabo and R. T. Sauer, *Annu. Rev. Biochem.*, 1992, **61**, 1053.
27 K. Yamasaki, T. Kigawa, M. Inoue, T. Yamasaki, T. Yabuki, M. Aoki, E. Seki, T. Matsuda, Y. Tomo, T. Terada, M. Shirouzu, A. Tanaka, M. Seki, K. Shinozaki and S. Yokoyama, *FEBS Lett.*, 2006, **580**, 2109.
28 R. P. Birkenbihl, G. Jach, H. Saedler and P. Huijser, *J. Mol. Biol.*, 2005, **352**, 585.
29 J. J. Storhoff, R. Elghanian, R. C. Mucic, C. A. Mirkin and R. L. Letsinger, *J. Am. Chem. Soc.*, 1998, **120**, 1959.
30 X. Zhang, M. R. Servos and J. Liu, *J. Am. Chem. Soc.*, 2012, **134**, 7266.
31 A. Opdahl, D. Y. Petrovykh, H. Kimura-Suda, M. J. Tarlov and L. J. Whitman, *Proc. Natl. Acad. Sci. U. S. A.*, 2007, **104**, 9.
32 H. Pei, F. Li, Y. Wan, M. Wei, H. Liu, Y. Su, N. Chen, Q. Huang and C. Fan, *J. Am. Chem. Soc.*, 2012, **134**, 11876.
33 M. Jeong, J. Park, H. Kim, J. Lee, A. Lee, Y. Choi and J. Lee, *Bull. Korean Chem. Soc.*, 2013, **34**, 2511.

